SAND2013-6956C

Development of CMOS-Compatible Membrane Projection Lithography

D. Bruce Burckel*[a], Sally Samora[a], Mike Wiwi[a], Joel R. Wendt[a]
[a]Sandia National Laboratories, P.O. Box 5800, Albuquerque, NM 87185

ABSTRACT

Recently we have demonstrated membrane projection lithography (MPL) as a fabrication approach capable of creating 3D structures with sub-micron metallic inclusions for use in metamaterial and plasmonic applications using polymer material systems. While polymers provide several advantages in processing, they are soft and subject to stress-induced buckling. Furthermore, in next generation active photonic structures, integration of photonic components with CMOS electronics is desirable. While the MPL process flow is conceptually simple, it requires matrix, membrane and backfill materials with orthogonal processing deposition/removal chemistries. By transitioning the MPL process flow into an entirely inorganic material set based around silicon and standard CMOS-compatible materials, several elements of silicon microelectronics can be integrated into photonic devices at the unit-cell scale. This paper will present detailed fabrication and characterization data of these materials, emphasizing the processing trade space as well as optical characterization of the resulting structures.

Keywords: Metamaterials, nanophotonics, 3D fabrication

1. INTRODUCTION

Fabrication of fully three dimensional structures at the micrometer scale is a challenging endeavor. Progress toward potentially transformative technologies such as metamaterials and next generation structured electromagnetic materials have been slowed due to the enormous difficulties in fabrication of the structures and geometries required at relevant size scales. For some time now, planar fabrication techniques have been used in a layer-by-layer fashion to create quasi-3D structures at the cost of a tedious fabrication process [1,2]. Recently a small subset of 3D fabrication techniques have emerged, such as direct laser write (DLW) [3], nano-origami [4], and membrane projection lithography[5-7], which are capable of creating a wide variety of differing structures by combining the fundamental process with additional processing steps.

Membrane projection lithography (MPL) is a 3D fabrication approach which uses standard cleanroom processing equipment combined with directional deposition to create 3D metallo-dielectric structures at the micron and sub-micron size scales. The basic fabrication sequence involves creating a suspended patterned membrane over a unit cell with three-dimensional topography (cubic, pyramidal, cylindrical spheroidal, etc), and then performing directional deposition(s) of metal through the patterned membrane onto the underlying topography. The result is a high fidelity reproduction of the membrane pattern projected onto the surface(s) of the unit cell. In this manner, micron-scale versions of the Pendry cube were created that were 1000 times smaller than their microwave counter parts, exhibiting an unambiguous magnetic resonance for a normally incident TEM wave due to the 3D nature of the unit cell. The MPL process flow used to create the Pendry cubes was an all-polymer approach, where the materials used to form the unit cells, backfill material and membrane were all polymeric. While this approach has several fabrication benefits including use of standard “low-tech” equipment and simplicity of process, working with an all polymer system presents several challenges, which make identifying a more rugged material set with inorganic materials compatible with the MPL process flow desirable. This paper describes our preliminary progress toward using dry etching to create cubic unit cells in silicon as the matrix material.

The top row of Fig. 1 contains a schematic sequence of panels showing the membrane projection lithography process, while the bottom row contains SEM images showing cross section images taken at various stages of the fabrication process. In this instance, the entire process uses organic polymers for each of the component materials of matrix (SU-8), backfill (polyimide) and membrane (PMMA). Once cross-linked and hardbaked, the SU-8 is relatively immune to chemical attack. The polyimide used as the backfill and planarization material is a commercially available polyimide which, when baked below its immidization temperature, remains soluble in

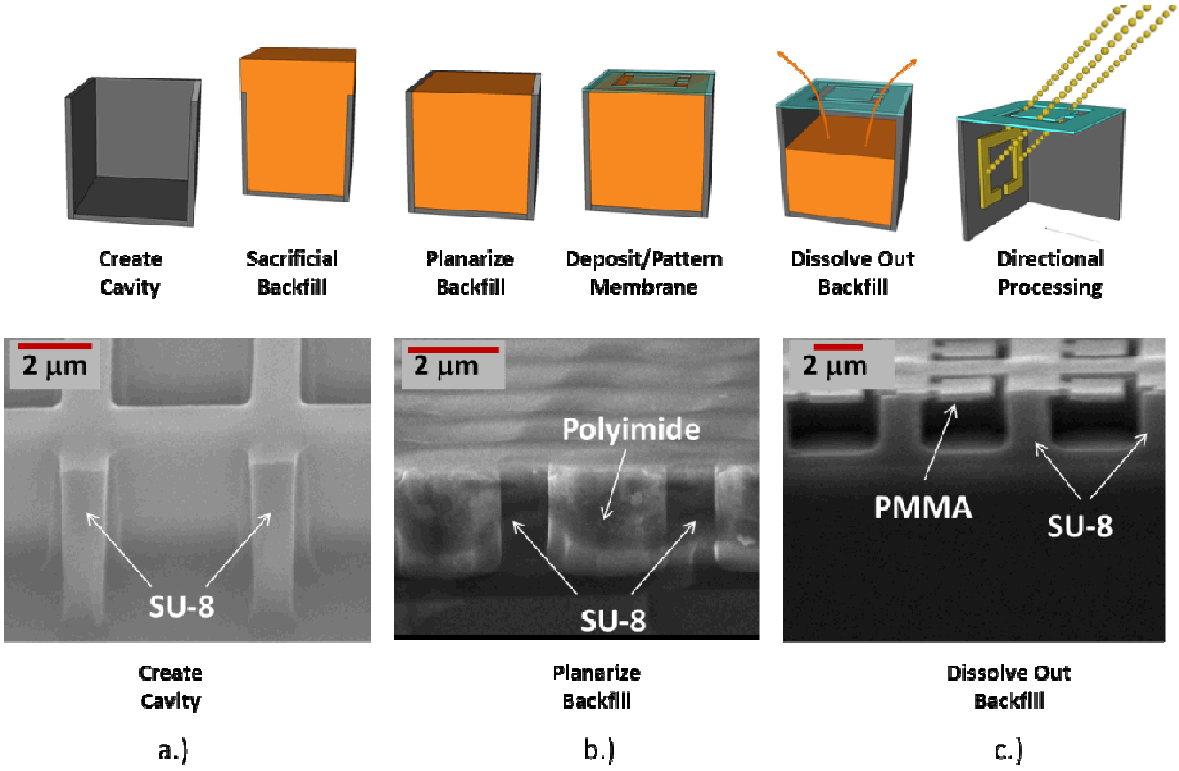

Fig. 1. (Top) Schematic depiction of the generic membrane projection lithography fabrication process. (Bottom) Cross-section SEM image sequence of three stages of MPL process flow.

standard TMAH-based photoresist developer, but is resistant to solvents. After over-coating the SU-8 unit cell array, the polyimide is etched back in an O2 plasma to the level of the SU-8 boxes, and the PMMA is spin-coated and patterned using electron beam lithography (EBL) and development in methyl isobutyl ketone (MIBK). At this point, the TMAH-based developer is used to dissolve out the polyimide backfill yielding a patterned suspended membrane over the cube shaped unit cell. Despite the fact that the polyimide is dissolved out and removed from the cavity through the patterned membrane, the PMMA maintains structural integrity remarkably well. The slight droop in the rightmost unit cell is a consequence of charging during imaging.

2. ISSUES WITH POLYMER MATERIAL SETS FOR MPL

2.1 Matrix material relaxation

Exposure of these relatively high aspect ratio unit cells with 1 micrometer thick walls thorugh a mask is a challenging lithography task, requiring highly optimized exposure parameters, which tend to favor barely cross-linked patterns in order to resolve the features. After exposure and development of the SU-8 unit cells, it is necessary to flood expose and hardbake the SU-8 structure to completely cross-link the material. Several downstream steps involve extensive exposure to solvents which can affect the SU-8 structure. For instance, the next step is the deposition of alignment marks to assist in etchback end-point-detection and e-beam pattern aligment. This step involved coating the boxes with i-Line photoresist, patterneing, metal deposition and acetone liftoff. In addition, both the polyimide backfill and PMMA membrane are organic polymers which are dissolved in organic solvents. Finally after deposition of the resonators onto the sidewalls, the metal coated PMMA membrane is removed using actetone immersion and acetone spray. The dominant failure mechanism of these polymer unit cell arrays is a relaxation of the walls during subsequent processing. The result is shown in Fig. 2. The unit cell array is a square array as drawn on the mask, and after exposure and develop of the boxes, remains so. In Fig. 2a, it is apparent that the region coated in gold as an end-point-detector region retains its square geometry, while hints of relaxation are

apparent in the non-gold-coated regions. In Fig. 2b. the samples have been backfilled, planarized, the PMMA membrane patterned and the backfill removed. The relaxation to a tiled rectangular geometry is obvious. Remarkably, while the unit cell geometry changes from a symmetric square to the tiled rectangular one, the e-beam

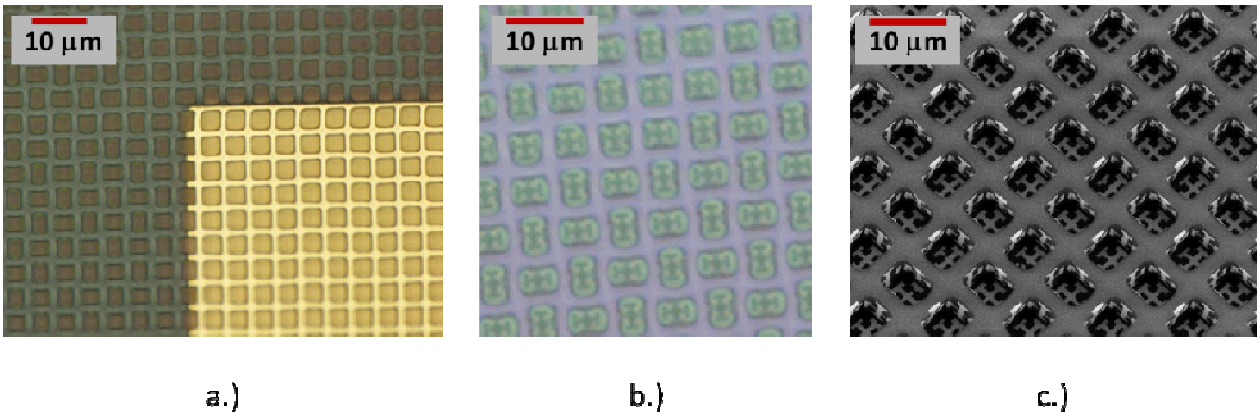

Fig. 2. SU-8 unit cell matrix relaxation. a.) Top-down optical image showing relaxation – gold coated alignment mark boxes retain a square shape while uncoated boxes relax to a tiled-rectangular array; b.) Top-down optical image of patterned membrane over relaxed unit cells; c.) Tilted SEM image after evaporation – presence of gold on tops of boxes is due to evaporation along the minor axis of the rectangular unit cell where the pattern no longer fits in the cell.

written pattern, which is laid out relative to the centers of the square unit cells, still possesses perfect alignment to the center of the rectangular cells. Despite this excellent alignment, the fact that MPL is a geometrical process severely affects the final evaporated patterns. In Fig. 2c. it is apparent that when the evaporation occurs along the major axis of a unit cell, the pattern lands on the opposing wall lower than intended, while when the evaporation occurs along the minor axis of the unit cell, the pattern lands higher on the opposing wall, and sometimes does not fit in the unit cell, but drapes along the top of the unit cell wall.

2.2 Polyimide bubble formation

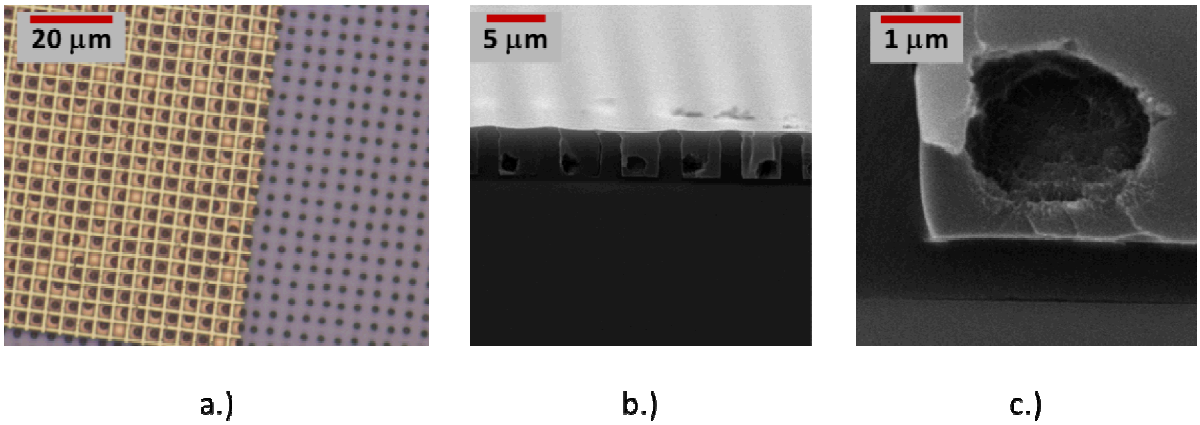

Fig 3. Polyimide bubble formation. a.) Top-down optical image indicating presence of bubbles in polyimide backfill; b.) Cross-section SEM image of layer indicating bubbles occur exclusively at the bottom of the unit cell; c.) High-magnification SEM image of polyimide bubble.

In an effort to address the SU-8 matrix relaxation, we increased the hardbake temperature and time. This approach helped in reducing the unit cell relaxation significantly, however it exposed a new peculiarity in the process. Fig. 3a. shows a top-down optical microscope image of backfilled boxes near a gold coated alignment mark. The black dots which appear in each unit cell are bubbles in the polyimide backfill. Because the polymers are transparent, it is not

possible to discern whether the bubbles are located on the surface, in the interior of the unit cell, or a mixture of these behaviors. From cross-section SEMs (Fig. 3 b-c) it is apparent that the bubbles form exclusively on the bottoms of the unit cells, and hence do not pose a problem.

Although the increased hard-bake conditions helped alleviate the unit-cell relaxation behavior, under certain conditions the SU-8 unit cells would still buckle, forcing us to scrap material. We also have a more general interest in transitioning this fabrication approach to inorganic materials to increase the ruggedness of the parts, avoid the midwave/longwave IR absorption bands of the organic polymer matrix and move into material sets which are inherently CMOS compatible. For this reason, we have begun investigating shifting to a silicon matrix material. As a first step, we attempted to use a silicon matrix, but retain the use of the polyimide backfill and PMMA membrane material choices.

3. MIGRATION TO INORGANIC MATRIX

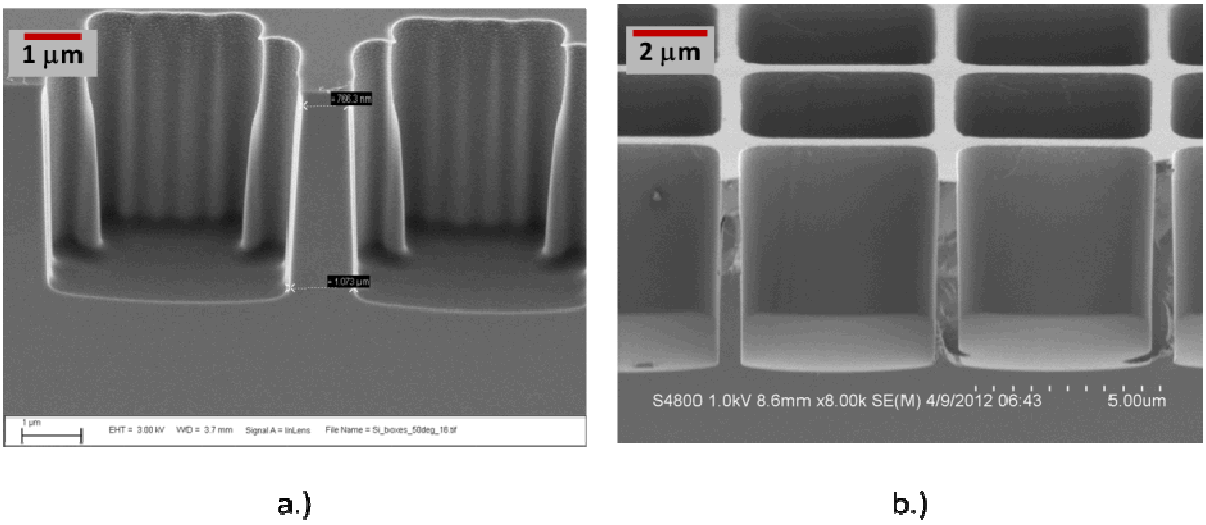

Fig. 4. Contact lithography to generate silicon unit-cells. a.) Sub-optimal exposure parameters and poor contact lead to notching, curtaining and loss of fidelity; b.) Optimized exposure and etch paramters can yield high quality boxes.

The first step in transitioning to an inorganic matrix material is establishing the method to create the unit cells. While the SU-8 material is photo-lithographically patternable, creating the unit cell walls in an additive process, silicon is not photopatternable, so that the unit cells must be etched, creating the cavity in a subtractive process. Fig. 4a. shows an etched unit-cell where the contact lithography used to pattern the etch mask suffered from poor contact and subsequent diffraction. This sub-optimality in the exposure was faithfully reproduced in the etch process. In the example unit cell shown in Fig. 4b. the exposure issues were remedied, resulting in significantly improved unit-cell properties, with high aspect ratio walls with only a slight taper.

Starting from etched silicon unit cells, we then proceeded to use the polyimide backfill to planarize the unit-cells. Fig. 5a. shows a top-down SEM image of a backfilled and etched back unit cell. At the periphery of the unit cell, a gap is apparent between the polyimide "plug" and the silicon unit-cell wall. In Fig. 5b. a planarized, but incompletely etched back unit-cell, shows both the polyimide bubbles forming at the bottom of the unit cell fill, as well as the presence of the gap between the silicon and polyimide. The fact that this gap is present even in under etched unit cells, indicates there is a fundamental material issue which must be resolved in order to use polyimide as the sacrificial backfill material in these unit-cells.

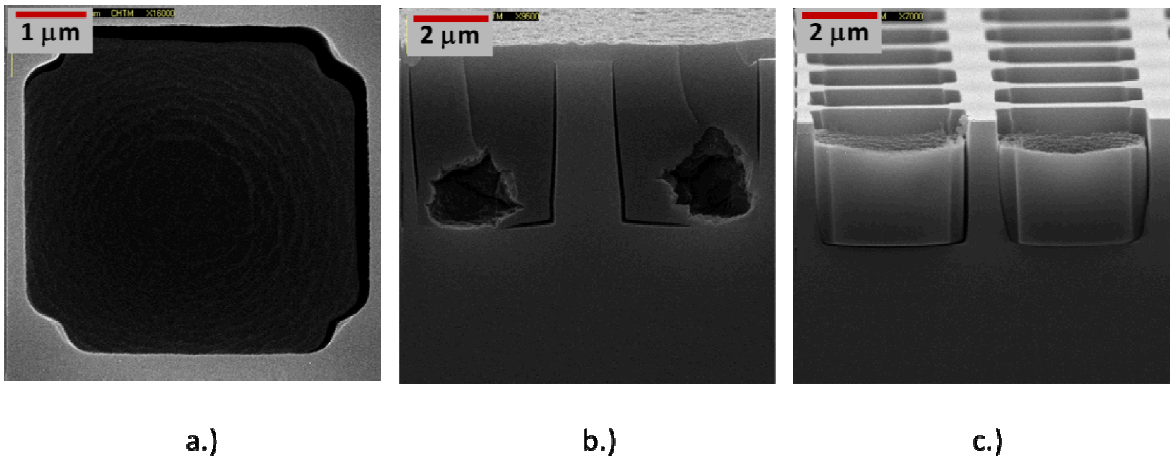

Fig. 5. SEM images of silicon unit cells backfilled with polyimide. a.) Top-down image showing exposed silicon walls with a large gap formed between silicon wall and polyimide backfill. b.) Cross-section SEM showing incompletely planarized unit cells. As in the polymer case the bubbles in the polyimide form at the bottom of the box, and the gap is evident even though the etchback is incomplete. c.) Cross-section SEM image of over etched backfilled boxes.

Fig. 6 shows several SEM images which demonstrate how the polyimide gap manifests itself as a collection of failure mechanisms in subsequent processing operations. In Fig 6a, a region of unit-cells which have been patterned with split ring resonators. A large fraction of the patterned membranes covering the unit cells have completely detached from the unit-cell, and those that remain suffer from splits occurring at the unit-cell periphery. It is possible that these failures are due to the flux of dissolved polyimide, however the top-down SEM image in Fig. 6b. indicates that this is not the cause of the failures as even regions with no patterneing, and hence should h ave had no flux of developer/dissolved polyimide exhibit similar splits at the unit-cell wall boundaries. Finally, in Fig 6c. an SEM image of an evaporated 4-split SRR shows a gossamer thin layer upon which the SRR has been evaporated onto. Analysis of these failure mechanisms is presented below.

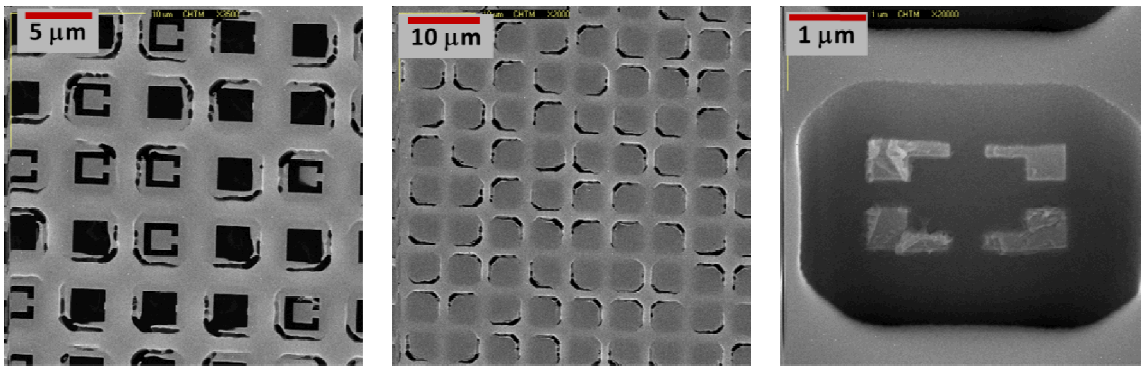

Fig. 6. Failure mechanisms in MPL using a silicon matrix with polyimide backfill. a.) Top down SEM image of patterned PMMA membranes over unit cells with the polyimide dissolved out; b.) Top-down SEM image of unpatterned PMMA membranes over unit cells with clear evidence of membrane failure; c.) Angled SEM image of an evaporated 4-gap split ring resonator showing the filmy residue of PMMA on the evaporated pattern.

4. RESULTS AND CONCLUSIONS

The success of the MPL fabrication approach depends critically on finding process-orthogonal material sets for the matrix, backfill and membrane materials. In the all-polymer system, this is accomplished by selecting an SU-8 matrix material, polyimide backfill and PMMA membrane. While successful at demonstrating proof-of-concept of the MPL approach, this all-polymer material set suffered from relaxation of the cubic matrix, into a tiled rectangular matrix after deposition and patterning of the PMMA membrane. Attempts to transition this process flow to a CMOS-compatible material set in a step-wise fashion, by replacing the lithographically patterned SU-8 matrix with an etched silicon matrix were successful in resolving the matrix relaxation issues, but uncovered failure mechanisms which were not identified in the all polymer system, the most troublesome being the formation of a gap between the silicon unit-cell walls and the polyimide backfill material. Although this gap is < 100 nm, it resulted in degradation of the PMMA membrane film as well as penetration of PMMA into the gap and subsequent deposition on the wall. The weakening of the PMMA membrane was present in both patterned (Fig. 6a.) and unpatterned (Fig. 6b.) unit cells, while the presence of the PMMA film on the wall resulted in a detectable gossamer polymer layer on the wall (Fig. 6c.) and lack of adhesion on subsequent evaporation.

Several attempts were made to adjust the post-apply bake temperatures and times of the polyimide layer, varying the temperature from 60 C – 250 C, with no noticeable effect on the gap size or prevalence. Given the long track history of backfilled MEMS-based fabrication, we are confident that these problems can be addressed using an entirely inorganic system, but the convenience and added flexibility of having a polymer backfill remains appealing. In future attempts, we will explore the success of alternative strategies for using a polyimide backfill in a silicon matrix by further adjusting backfill application and bake conditions, exploring two step deposition processes and new approaches to etchback.

ACKNOWLEDGEMENTS

Supported by the Laboratory Directed Research and Development program at Sandia National Laboratories. Sandia National Laboratories is a multiprogram laboratory managed and operated by Sandia Corporation, a Lockheed Martin Corporation, for the United States Department of Energy's National Nuclear Security Administration under Contract DE-AC04-94AL85000. Sand No. 2013-6956C.

REFERENCES

[1] Liu, N., Guo, H., Fu, L., Kaiser, S., Schweizer, H., and Giessen, H.,"Three-dimensional photonic metamaterials at optical frequencies," Nat. Mater. 7, 31-37 (2008).

[2] Valentine, J. , Zhang, S., Zentgraf, T., Ulin-Avila, E., Genov, D., A., G. Bartal, and Zhang, X., "Three-dimensional optical metamaterial with a negative refractive index," Nature 455, 376-380 (2008).

[3] Gansel, J.K., Thiel, M., Rill, M. S., Decker, M., Bade, K., Saile, V., von Freymann, G., Linden, S. and Wegener, M., "Gold helix photonic metamaterial as broadband circular polarizer," Science 325, 1513-1515 (2009).

[4] J.H. Cho, M.D. Keung, N. Verellen, L. Lagae, V.V.Moshchalkov, P. Van Dorpe, and D.H. Gracias, "Nanoscale Origami for 3D Optics," Small, 7, 1943-1948 (2011).

[5] D. B. Burckel, J. R. Wendt, G. A. Ten Eyck, A. R. Ellis, I. Brener, M. B. Sinclair, "Fabrication of 3D metamaterial resonators using self-aligned membrane projection lithography," Adv. Mat. 22, 3171-3175, (2010).

[6] D. B. Burckel, J. R. Wendt, G. A. Ten Eyck, A. R. Ellis, I. Brener, M. B. Sinclair, "Micrometer-scale cubic unit cell 3D metamaterial layers,"Adv. Mat. 22, 5053-5057 (2010).

[7] D.B. Burckel, J. R. Wendt, I. Brener, and M.B. Sinclair, "Dynamic Membrane Projection Lithography," Opt. Mater. Exp., 1, 962-969 (2011).